ORGANOMETALLICS

Article

pubs.acs.org/Organometallics

Asymmetric Catalyzed Allylic Substitution Using a Pd/P−S Catalyst Library with Exceptional High Substrate and Nucleophile Versatility: DFT and Pd-π-allyl Key Intermediates Studies

Jèssica Margalef,[†] Mercè Coll,[†] Per-Ola Norrby,[*,‡,§] Oscar Pàmies,[*,†] and Montserrat Diéguez[*,†]

[†]Departament de Química Física i Inorgànica, Universitat Rovira i Virgili, C/Marcel·lí Domingo 1, 43007 Tarragona, Spain

[‡]Pharmaceutical Sciences, AstraZeneca, Pepparedsleden 1, SE-431 83 Mölndal, Sweden

[§]Department of Chemistry and Molecular Biology, University of Gothenburg, Kemigården 4, SE-412 96 Göteborg, Sweden

Supporting Information

ABSTRACT: A large library of furanoside phosphite/phosphinite/phosphine-thioether ligands **L1−L17a−l** has been applied in the Pd-catalyzed allylic substitution reactions of several substrate types using a wide range of nucleophiles. These ligands, which are prepared from inexpensive D-xylose, also incorporate the advantages of the heterodonor, the robustness of the thioether moiety, and the extra control provided by the flexibility of the chiral pocket through the presence of a biaryl phosphite group and a modular sugar backbone. By selecting the ligand components, we have been able to identify catalytic systems that can create new C−C, C−N, and C−O bonds in several substrate types (hindered and unhindered) using a wide range of nucleophiles in high yields and enantioselectivities (ee's up to >99%). Of particular note are the excellent enantioselectivities obtained in the etherification of linear and cyclic substrates, which represent the first example of successful etherification of both substrate types. The DFT computational study is in agreement with an early transition state. Further studies on the Pd-π-allyl intermediates provided a deep understanding of the effect of ligand structure in the origin of enantioselectivity.

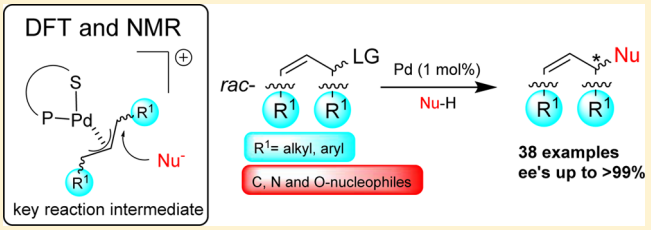

INTRODUCTION

Transition-metal-based asymmetric catalysis is a reliable, selective, and atom-economic strategy to access optically pure compounds. Remarkable efforts have been dedicated to the enantioselective Pd-catalyzed allylic substitution as one of the most relevant methods for creating C−C and C−heteroatom bonds.[1] Over the last decades, a great number of ligands have been successfully applied in this process. Most of these ligands are equipped with strong and weak donor heteroatom pairs (e.g., P−N, P−S, P−P′, etc.), which take advantage of the different *trans* influence of the two coordinative groups.[1] In this context, our group has contributed with a new generation of advanced ligands. We have found that biaryl π-acceptor groups (phosphite or phosphoroamidite moieties) in the ligands have an extremely positive effect on substrate versatility and activity.[1j,2] Despite all the remarkable advances in catalyst design, most of the ligands still rarely tolerate a broad range of substrates, and each type of substrate requires a particular ligand to optimize enantiopurity. Additional efforts are also required to widen the range of nucleophiles. Many important nucleophiles still provide suboptimal results with known catalysts. The discovery of more efficient catalysts, suited for a broad range of substrate and nucleophiles, is key for achieving the sustainable production of all the sorts of C−C and C−heteroatom bonds required for synthesizing more complex organic reactions in near future. Among heterodonor ligands, the mixed P-oxazoline ligands have played a dominant role. To a lesser extent, P-thioether ligands have also demonstrated their potential utility in Pd-catalyzed asymmetric allylic substitution.[3] The pioneering work of the groups of Pregosin[4] and Evans,[3a] among others, with P-thioether ligands in Pd-allylic substitution and other relevant asymmetric processes put the focus on these types of ligands and spur their development. Despite many P−S ligands being developed, only a few of them were successfully applied, and their efficiencies were limited in substrate scope (enantioselectivities were only high in the allylic substitution of hindered standard substrate *rac*-1,3-diphenyl-3-acetoxyprop-1-ene).[3] Compared to other functional groups, the thioether-based ligands have been less used because mixtures of diastereomeric thioether complexes are produced and because it is difficult to control their interconversion in solution.[5] Nevertheless, if the ligand scaffold can control the S-coordination, then this feature may be extremely beneficial because then the chirality moves closer to the metal. In this respect, we recently identified a simple ligand backbone that can control thioether coordination in Pd/phosphite-thioether catalysts. Our preliminary results showed than xylofuranoside phosphite-thioether ligands can be successfully applied in the Pd-catalyzed allylic substitution of several substrates types using

Received: July 7, 2016

DOI: 10.1021/acs.organomet.6b00547
Organometallics XXXX, XXX, XXX−XXX

several nucleophiles.[6] Despite this success, a systematic study of the scope of P,S-ligands is still needed. Moreover, no mechanistic studies exist about these ligands that can predict *a priori* the right ligand that will provide a high enantioselectivity. Therefore, more research is also required to discern the role of ligand parameters in the origin of enantioselectivity.

To investigate these possibilities, in this paper we expand the previous study of 2014[6] to other furanoside phosphite-thioether ligands (Figure 1) and also extent the study of these ligands to

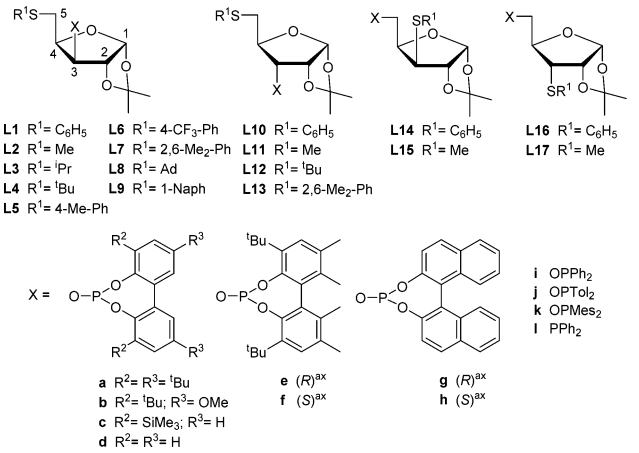

Figure 1. Phosphite/phosphinite/phosphine-thioether ligand library **L1**−**L17a**−**l**.

other substrates and nucleophiles. To do so, we have taken advantage of the high modularity of these sugar-based ligands and have synthesized and screened a library of potential 204 furanoside phosphorus-thioether ligands starting from the same underlying structure (Figure 1). We have therefore added two new ligand backbones (ligands **L14**−**L15** and **L16**−**L17**) to the Pd−P,S catalyst library, thus completing a two-level two-factor design with the four diastereomers that can be obtained by varying the configuration of C3 and the position of the thioether groups at either C5 and C3 of the furanoside backbone. This design allowed a comparative study of the effects of these configurations and of the position of the thioether group, as well as to discover any cooperative effects between them.

We have also enlarged the whole catalyst library by adding new substituents in the thioether and biaryl phosphite group. Finally, we also compare the effectiveness of these phosphite-thioether ligands with the related phosphinite-thioethers (**L1**−**L17i**−**k**) and phosphine-thioethers (**L1**−**L17l**). By varying these ligand parameters, we achieved high enantioselectivities and activities in a large number of hindered and unhindered substrates using a wide range of C-, N-, and O-nucleophiles. We have also extended the use of these new catalytic systems in propylene carbonate as alternative environmentally friendly solvent. In this paper we have also carried out DFT calculations and the synthesis of the Pd-π-allyl intermediates in order to explain the origin of enantioselectivity.

RESULTS AND DISCUSSION

Allylic Substitution of Disubstituted Substrates S1−**S3 Using Dimethyl Malonate as Nucleophile.** As mentioned previously, asymmetric Pd-catalyzed allylic substitution is highly dependent on the steric demands of the substrate. Enantioselectivity is lower for unhindered substrates than for the corresponding hindered substrates. To evaluate the phosphite/phosphinite/phosphine-thioether ligands **L1**−**L17a**−**l** in the Pd-allylic substitution of substrates with different steric properties, we initially tested the ligands in the substitution of the hindered substrate *rac*-1,3-diphenyl-3-acetoxyprop-1-ene **S1** and that of two unhindered substrates *rac*-3-acetoxycyclohexene **S2** and *rac*-1,3-dimethyl-3-acetoxyprop-1-ene **S3** (eq 1). In all the cases, the catalysts were

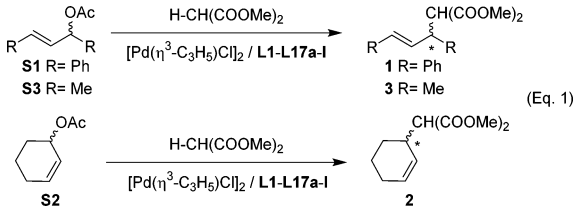

generated *in situ* from π-allyl-palladium chloride dimer $[PdCl(\eta^3\text{-}C_3H_5)]_2$, the corresponding ligand, and the nucleophile. The results (Table 1) indicate that enantioselectivity varies considerably depending on the position of the thioether group in the furanoside backbone, the configuration of C3, the thioether substituents, and the substituents/configuration in the biaryl phosphite moiety (**a**−**h**), as well as whether the phosphite moiety is replaced by a phosphinite (**i**−**k**) or a phosphine (**l**) group.

The results indicate a cooperative effect between the position of the thioether group and the configuration of carbon atom C3 of the furanoside backbone (Table 1, entries 1, 12, 31, 34, 39, 43, and 44). While for substrates **S1** and **S2** the matched combination is achieved with 5-deoxy-xylofuranoside derived ligands **L1**−**L9** (which have the thioether at C5 of the furanoside backbone and whose carbon atom C3 has an *S* configuration), for substrate **S3** the matched combination is achieved with 5-deoxy-ribofuranoside derived ligands **L10**−**L13**. It should be pointed out when the thioether group was attached to C3 (ligands **L14**−**L17**; entries 39−44) the enantioselectivity was lower than when the thioether moiety was attached to C5. This suggests that the furanoside backbone controls better the thioether inversion when the thioether group is attached to C5 (flexible primary carbon) rather to the stereogenic secondary carbon C3. This unexpected behavior proves the relevance of using highly modular scaffold to make new ligands.

The effects of the phosphite moiety were studied with the 5-deoxy-xylofuranoside ligands **L1a**−**h** (Table 1, entries 1−8). We found that enantioselectivity increased with bulky substituents at the *ortho* positions of the biaryl phosphite moieties (i.e., entries 1−3 vs 4) but was hardly changed by the nature of the substituents at the *para* positions of the biaryl phosphite group (entries 1−3). The results also show a cooperative effect between the configuration of the bulky biphenyl moiety and the configurations of the ligand backbone. This led to a matched combination for ligand **L1f**, which contains an *S*-biaryl moiety (entry 6). Nevertheless, the cooperative effect using 5-deoxy-ribofuranoside ligands **L13e**,**f** led to a matched combination for ligand **L13e**, containing an *R*-biaryl moiety (entry 37). The results also indicated that to obtain high enantioselectivities an *S* configuration of the biaryl phosphite moiety must be adopted for substrates **S1** and **S2** (entries 6, 21, and 29) while an *R* configuration is needed for substrate **S3** (entries 32 and 37).

DOI: 10.1021/acs.organomet.6b00547
Organometallics XXXX, XXX, XXX−XXX

Table 1. Pd-Catalyzed Allylic Alkylation of S1−S3 with Dimethyl Malonate Using the Ligand Library L1−L17a−l[a]

		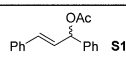 S1		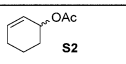 S2		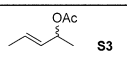 S3	
Entry	Ligand	% Conv (h)[b]	% ee[c]	% Conv (h)[b]	% ee[c]	% Conv (h)[b]	% ee[c]
1	**L1a**	100 (3)	58 (*S*)	100 (3)	78 (*S*)	100 (3)	57 (*S*)
2	**L1b**	100 (3)	63 (*S*)	100 (3)	77 (*S*)	100 (3)	55 (*S*)
3	**L1c**	100 (3)	54 (*S*)	100 (3)	78 (*S*)	100 (3)	56 (*S*)
4	**L1d**	100 (3)	2 (*R*)	100 (3)	3 (*S*)	100 (3)	4 (*R*)
5	**L1e**	100 (3)	20 (*R*)	100 (3)	63 (*S*)	100 (3)	19 (*S*)
6	**L1f**	100 (3)	95 (*S*)	100 (3)[d]	96 (*S*)	100 (3)	68 (*S*)
7	**L1g**	100 (3)	10 (*R*)	100 (3)	4 (*R*)	100 (3)	2 (*R*)
8	**L1h**	100 (3)	9 (*S*)	100 (3)[d]	5 (*S*)	100 (3)	4 (*S*)
9	**L1i**	100 (3)	63 (*S*)	100 (3)	4 (*R*)	100 (3)	7 (*R*)
10	**L1j**	100 (3)	63 (*S*)	100 (3)[d]	45 (*S*)	100 (3)	24 (*S*)
11	**L1k**	100 (3)	54 (*S*)	100 (3)	28 (*S*)	100 (3)	29 (*S*)
12	**L2a**	100 (3)	63 (*S*)	100 (3)	68 (*S*)	100 (3)	47 (*S*)
13	**L3a**	100 (3)	54 (*S*)	100 (3)	52 (*S*)	100 (3)	34 (*S*)
14	**L4a**	100 (3)	49 (*S*)	100 (3)	44 (*S*)	100 (3)	4 (*R*)
15	**L4i**	100 (3)	86 (*S*)	100 (3)	75 (*S*)	100 (3)	33 (*R*)
16	**L4j**	100 (3)	70 (*S*)	100 (3)	48 (*R*)	100 (3)	9 (*S*)
17	**L5a**	100 (3)	59 (*S*)	100 (3)	77 (*S*)	100 (3)	56 (*S*)
18	**L6a**	100 (3)[d]	57 (*S*)	100 (3)	75 (*S*)	100 (3)	54 (*S*)
19	**L7a**	100 (3)	69 (*S*)	100 (3)	63 (*S*)	100 (3)	63 (*S*)
20	**L7e**	100 (3)	52 (*R*)	100 (3)	63 (*S*)	100 (3)	16 (*S*)
21	**L7f**	100 (3)	98 (*S*)	100 (3)	92 (*S*)	100 (3)	72 (*S*)
22	**L7l**	100 (3)	15 (*S*)	100 (3)	5 (*R*)	100 (3)	4 (*R*)
23	**L8a**	100 (3)	78 (*S*)	100 (3)	48 (*S*)	100 (3)	7 (*S*)
24	**L8e**	100 (3)[d]	35 (*R*)	100 (3)	40 (*R*)	100 (3)	3 (*S*)
25	**L8f**	100 (3)	84 (*S*)	100 (3)	86 (*S*)	100 (3)	35 (*S*)
26	**L8i**	100 (3)	58 (*S*)	100 (3)	60 (*R*)	100 (3)	44 (*S*)
27	**L9a**	100 (3)	78 (*S*)	100 (3)	75(*S*)	100 (3)	68 (*S*)
28	**L9e**	100 (3)[d]	33 (*R*)	100 (3)	32 (*S*)	100 (3)	17 (*S*)
29	**L9f**	100 (3)	>99 (*S*)	100 (3)	96 (*S*)	100 (3)	76 (*S*)
30	**L9i**	100 (3)	60 (*S*)	100 (3)	27 (*S*)	100 (3)	55 (*S*)
31	**L10a**	100 (3)	53 (*R*)	100 (3)	41 (*R*)	100 (3)	39 (S)
32	**L10e**	100 (3)[d]	51 (*R*)	100 (3)	49 (*R*)	100 (3)	88 (S)
33	**L10f**	100 (3)	24 (*S*)	100 (3)	19 (*S*)	100 (3)	8 (S)
34	**L11a**	100 (3)	52 (*R*)	100 (3)	41 (*R*)	100 (3)	49 (*S*)
35	**L12a**	100 (3)[d]	13 (*S*)	100 (3)	9 (*R*)	100 (3)	12 (*R*)
36	**L13a**	100 (3)	60 (*R*)	100 (3)	66 (*S*)	100 (3)	48 (S)
37	**L13e**	100 (3)[d]	64 (*R*)	100 (3)	62 (*R*)	100 (3)	96 (*S*)
38	**L13f**	100 (3)	11 (*S*)	100 (3)	24 (*S*)	100 (3)	7 (*S*)
39	**L14a**	100 (3)[d]	12 (*S*)	100 (3)	24 (*S*)	100 (3)	18 (*S*)
40	**L14e**	100 (3)[d]	36 (*S*)	100 (3)	24 (*S*)	100 (3)	9 (*S*)
41	**L14f**	100 (3)	29 (*R*)	100 (3)	57 (*S*)	100 (3)	32 (*S*)
42	**L15a**	100 (3)	32 (*R*)	100 (3)	40 (*R*)	100 (3)	20 (*R*)
43	**L16a**	100 (3)[d]	9 (*R*)	100 (3)	4 (*S*)	100 (3)	8 (*S*)
44	**L17a**	100 (3)	4 (*R*)	100 (3)	3 (*S*)	100 (3)	3 (*S*)

[a]0.5 mol % $[PdCl(\eta^3\text{-}C_3H_5)]_2$, ligand (0.011 mmol), **S1−S3** (1 mmol), CH_2Cl_2 (2 mL), BSA (3 equiv), dimethyl malonate (3 equiv), KOAc (5 mol %), rt. [b]Conversion percentage determined by ^{1}H NMR (for **S1**) or GC (for **S2** and **S3**). [c]Enantiomeric excesses determined by HPLC (for **S1**) and GC (for **S2−S3**). Absolute configuration drawn in parentheses. [d]Isolated yields ≥92%.

The effect of the phosphinite moiety was studied with ligands **L1i−k**. The results indicated that enantioselectivity was negatively affected by the steric bulk of the phosphinite group (entries 9−11). Thus, in general, ligands containing a mesityl phosphinite group provided the lowest enantioselectivites of the phosphinite series. Moreover, when we compared these results with those achieved with the phosphite (**L1a−h**) and phosphine (**L7l**; entry 22) counterparts, we observed that the best enantioselectivities were obtained with ligands containing a bulky *S*-biaryl phosphite moiety (ligand **L1f**).

DOI: 10.1021/acs.organomet.6b00547
Organometallics XXXX, XXX, XXX−XXX

The effect of the thioether substituent was studied with ligands **L1**−**L9** (Table 1). Results showed that an aryl thioether substituent is needed for high enantioselectivity. Thus, in general the highest enantioselectivities were achieved using a phenyl (ligands **L1**), 2,6-dimethylphenyl (ligands **L7**), or a 1-naphthyl (ligands **L9**) thioether groups.

In summary, the optimization of the ligand structure lead us to identify Pd/**L9f** and Pd/**L13e** as two of the very few Pd-catalysts that can provide excellent enantiocontrol for the substrates with different steric demands that we tested (ee's up to >99% for **S1** and **S2** with Pd/5-deoxy-xylofuranoside based ligand **L9f**, entry 29, and up to 96% for **S3** with Pd/using 5-deoxy-ribofuranoside ligand **L13e**, entry 37). These results compare favorably with the best ones reported in the literature.

Allylic Substitution of Disubstituted Substrates Using Several Nucleophiles: Scope and Limitations. We also studied the scope of the best catalytic systems (Pd-**L9f** for hindered linear substrate **S1** and unhindered cyclic substrate **S2**; Pd-**L13e** for unhindered linear substrate **S3**) considering other C-, N-, and O-nucleophiles and more substrates (Figure 2).

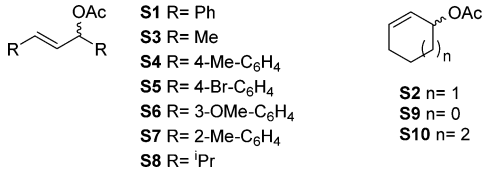

Figure 2. Substrates **S1**−**S10** used in this study.

We first studied the allylic substitution of **S1** with Pd-**L9f** catalyst using a variety of C-, N-, and O-nucleophiles (Table 2). Several malonates, including those substituted with allyl, butenyl, pentenyl, and propargyl groups, reacted efficiently with **S1** to afford products **4**−**10** in high yields and enantioselectivities (ee's up to 99%, entries 1−7) comparable to those obtained with dimethyl malonate. These results are highly relevant because compounds **7**−**10** are key intermediates for synthesizing more complex chiral molecules.[7] The reaction also worked well when the nucleophiles were acetylacetone (compound **11**, entry 8) and benzylamine (compound **14**, entry 11) (ee's up to >99%). The excellent enantiocontrol also extends to the use of malononitrile and isopropyl cyanoacetate (compounds **12** and **13**; ee's up to 99%, entries 9 and 10). The use of the isopropyl cyanoacetate resulted in the formation of two diastereoisomers in excellent ee's, albeit with low diastereoselectivity, like in previous reports.[8]

Aliphatic alcohols are other relevant nucleophiles that are receiving much attention. The allylic substitution with this type of O-nucleophiles opens up a path for obtaining aliphatic chiral ethers which are important for the synthesis of biologically active targets.[9] However, in contrast to the use of phenols as nucleophiles,[10] aliphatic alcohols have been less studied.[2g,3a,7c,11] Moreover, the results of the aliphatic alcohols to a larger extent depend on the type of alcohol, and simple modifications in its electronic properties can lead to important differences in enantioselectivity.[2g,3a,7c,11] Improving previous results, we found that Pd-**L9f** is quite robust to varying electronic properties of the nucleophile (Table 2, entries 12−16). A broad range of aliphatic alcohols reacted efficiently with **S1** to afford compounds **15**−**19** with excellent yields and enantioselectivities (ee's up to >99%). Our results surpass the best results with Pd-(*R*,*R*)-FerroNPS[11c] and Pd-CycloN2P2-Phos[11d] catalytic systems specifically designed for this purpose.

We also found that the biaryl phosphite group in Pd-**L9f** and Pd-**L13e** can adapt its chiral pocket and successfully catalyze other linear substrates **S3**−**S8** with different steric and electronic requirements (Table 2, entries 17−25). Advantageously, we found that the catalytic performance was not affected by either the introduction of *ortho*- and *meta*-substituents at the phenyl groups of the substrate **S1** or the introduction of electron-withdrawing and -donating groups (compounds **20** and **23**−**25**). The use of C-nucleophiles other than dimethyl malonate provides comparable excellent enantioselectivities. In the alkylation of the unhindered substrate **S3** using Pd-**L13e** catalytic system as observed using dimethyl malonate as nucleophile (Table 1), the use of other C-nucleophiles led to a lower but still remarkable enantioselectivity (ee's up to 90%, compounds **26** and **27**) for this challenging substrate. There are fewer successful catalysts for the Pd-catalyzed allylic substitution of **S3** than the allylic substitution of hindered **S1** due to the presence of less sterically demanding methyl *syn* substituents. Also, the Pd-allylic alkylation of substrate **S8**, which is more sterically demanding and is usually substituted much less enantioselectively than **S1**, also proceeded with high enantioselectivity (>95% ee; compound **28**, entry 25). These results are among the best in the literature for these substrates, even with synthetically useful nucleophiles other than dimethyl malonate, for which only very few catalytic systems have provided high enantioselectivities.

We completed the study by applying Pd-**L9f** in the allylic substitution of cyclic substrates with different ring size (**S2**, **S9**, and **S10**) with a range of C-, N-, and O-nucleophiles (Table 2, entries 27−35). Due to the presence of less bulky *anti*-substituents, the enantioselectivity for cyclic substrates is more difficult to control than for **S1**. The results show that enantioselectivities in the allylic alkylation of **S2** were as high as those obtained using dimethyl malonate (ee's up to 98%), except when the nucleophile was dimethyl methylmalonate, which led to a slightly lower enantioselectivity (compound **29**; 87% ee). Excellent ee's were therefore obtained using challenging allyl- and propargyl-substituted nucleophiles (compounds **30** and **31**), acetylacetone (compound **32**), and benzylamine (compound **33**). Even more remarkable are the high yields and enantioselectivities achieved in the etherification of **S2** (compound **34**). Pd-**L9f** is the first catalytic system that can etherificate both linear substrates **S1** (Table 2, compounds **15**−**19**) and cyclic substrates **S2** with high ee's (compound **34**, entry 31).[11a]

Advantageously, Pd-**L9f** could also provide excellent yields and enantioselectivities, comparable to the best ones reported in the literature with other cyclic substrates with a different ring size (entries 32−25). Pd-**L9f** also successfully catalyzed the allylic substitution of *rac*-3-acetoxycyclopentene (compounds **35** and **36**), which is usually substituted less enantioselectively than the 6-membered cyclic substrate **S2** thanks to the ability of the biaryl phosphite group to adapt its chiral pocket.

Encouraged by the excellent results, we went one step further and studied the Pd-catalyzed allylic substitution using 1,2-propylene carbonate (PC). PC has emerged as a sustainable "green" alternative to standard organic solvents because of its high boiling point, low toxicity, and environmentally friendly synthesis.[12] We repeated, using PC as solvent, the allylic substitution of substrates **S1**−**S10** with the ligands that provided the best enantioselectivities for each substrate and

DOI: 10.1021/acs.organomet.6b00547
Organometallics XXXX, XXX, XXX−XXX

Table 2. Pd-Catalyzed Allylic Alkylation of S1−S10[a]

Entry	Substrate	Product	% Yield	% ee[b]	Entry	Substrate	Product	% Yield	% ee[b]
1	**S1**	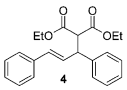 4	96	99 (*S*)	19	**S4**	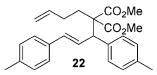 22	88	>99 (*R*)
2	**S1**	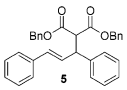 5	94	99 (*S*)	20	**S5**	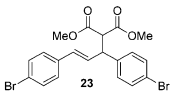 23	91	98 (*S*)
3	**S1**	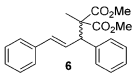 6	98	98 (*R*)	21	**S6**	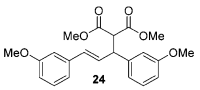 24	88	97 (*S*)
4	**S1**	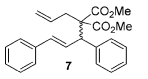 7	87	92 (*R*)	22	**S7**	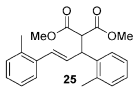 25	90	99 (*S*)
5	**S1**	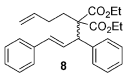 8	88	97 (*R*)	23[d]	**S3**	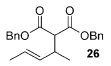 26	81	86 (*S*)
6	**S1**	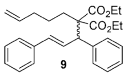 9	92	95 (*R*)	24[d]	**S3**	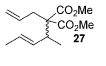 27	78	90 (*S*)
7	**S1**	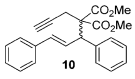 10	88	98 (*R*)	25	**S8**	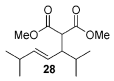 28	96	>95 (*S*)
8	**S1**	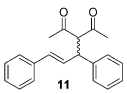 11	91	99 (*S*)	26	**S2**	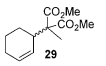 29	86	87 (*S*)
9	**S1**	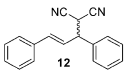 12	90	99 (*S*)	27	**S2**	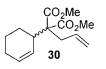 30	69	93 (*S*)
10	**S1**	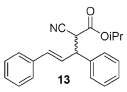 13	88 (55:45 dr)	98/95	28	**S2**	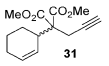 31	69	98 (*S*)
11	**S1**	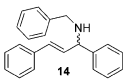 14	86	>99 (*R*)	29	**S2**	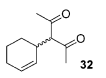 32	64	96 (*S*)
12[c]	**S1**	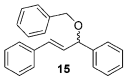 15	95	98 (*R*)	30	**S2**	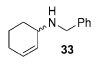 33	76	94 (*S*)
13[c]	**S1**	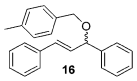 16	86	93 (*R*)	31[c]	**S2**	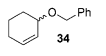 34	88	92 (*S*)
14[c]	**S1**	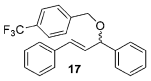 17	97	99 (*R*)	32	**S9**	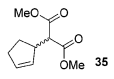 35	83	>95 (*S*)
15[c]	**S1**	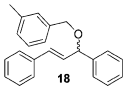 18	93	>99 (*R*)	33	**S9**	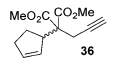 36	89	>99 (*S*)
16[c]	**S1**	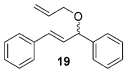 19	52	85 (*R*)	34	**S10**	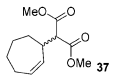 37	91	99 (*S*)
17	**S4**	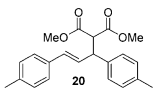 20	91	99 (*S*)	35	**S10**	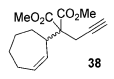 38	90	>99 (*S*)
18	**S4**	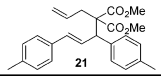 21	90	99 (*R*)					

[a]0.5 mol % $[PdCl(\eta^3\text{-}C_3H_5)]_2$, **L9f** (0.011 mmol), substrate (1 mmol), CH_2Cl_2 (2 mL), BSA (3 equiv), nucleophile (3 equiv), KOAc (5 mol %), 3 h, rt. [b]Enantiomeric excesses determined by HPLC or GC. Absolute configuration drawn in parentheses. [c]Reactions carried out using 2 mol % $[PdCl(\eta^3\text{-}C_3H_5)]_2$, 4 mol % ligand, Cs_2CO_3 (3 equiv) for 18 h. [d]Reactions carried out using **L13e** at 0 °C.

with various C- and N-nucleophiles. The results are collected in Table 3. We were pleased to see that the enantioselectivities with PC remained as high as those observed with dichloromethane for a wide range of nucleophiles and substrates types.

DOI: 10.1021/acs.organomet.6b00547
Organometallics XXXX, XXX, XXX−XXX

Table 3. Pd-Catalyzed Allylic Alkylation of S1−S10 Using Propylene Carbonate (PC) as Solvent[a]

entry	substrate	Nu−H (product)	% yield	% ee[b]
1	**S1**	H−CH(COOMe)$_2$ (**1**)	87	98 (*S*)
2	**S1**	H−CMe(COOMe)$_2$ (**6**)	88	97 (*R*)
3	**S1**	H−Callyl(COOMe)$_2$ (**7**)	90	92 (*R*)
4	**S1**	H−Cbutenyl(COOMe)$_2$ (**8**)	86	97 (*R*)
5	**S1**	H−Cpentenyl(COOMe)$_2$ (**9**)	87	94 (*R*)
6	**S1**	H−Cpropargyl(COOMe)$_2$ (**10**)	84	98 (*R*)
7	**S1**	H−CH(COMe)$_2$ (**11**)	90	98 (*S*)
8	**S1**	H−NHBn (**14**)	87	99 (*R*)
9	**S2**	H−CH(COOMe)$_2$ (**2**)	87	95 (*S*)
10	**S2**	H−Cpropargyl(COOMe)$_2$ (**31**)	78	98 (*S*)
11	**S2**	H−CH(COMe)$_2$ (**32**)	80	95 (*S*)
12[c]	**S3**	H−CH(COOMe)$_2$ (**3**)	81	94 (*S*)
13	**S4**	H−CH(COOMe)$_2$ (**20**)	87	98 (*S*)
14	**S4**	H−Callyl(COOMe)$_2$ (**21**)	85	98 (*R*)
15	**S5**	H−CH(COOMe)$_2$ (**23**)	81	97 (*S*)
16	**S6**	H−CH(COOMe)$_2$ (**24**)	83	97 (*S*)
17	**S7**	H−CH(COOMe)$_2$ (**25**)	86	99 (*S*)
18	**S8**	H−CH(COOMe)$_2$ (**28**)	82	>95 (*S*)
19	**S9**	H−CH(COOMe)$_2$ (**35**)	73	>95 (*S*)
20	**S10**	H−CH(COOMe)$_2$ (**37**)	83	98 (*S*)
21	**S10**	H−Cpropargyl(COOMe)$_2$ (**38**)	81	99 (*S*)

[a]0.5 mol % [PdCl(η^3-C_3H_5)]$_2$, **L9f** (0.011 mmol), substrate (1 mmol), CH_2Cl_2 (2 mL), BSA (3 equiv), nucleophile (3 equiv), KOAc (5 mol %), 40 °C, 3 h. [b]Enantiomeric excesses determined by HPLC or GC. Absolute configuration drawn in parentheses. [c]Reaction carried out using **L13e**.

Origin of Enantioselectivity. *DFT Computational Studies.* We performed a DFT computational study of the key intermediates and transition states involved in the enantiocontrol of the Pd-catalyzed allylic substitution of hindered substrate **S1** and unhindered substrate **S2**, using ligands **L9e** and **L9f** as models. These ligands contain two different biaryl phosphite groups that will help us understand the reason why bulky chiral biaryl phosphite moieties enhance enantioselectivity. The mechanistic studies found in the literature have shown that enantioselectivity is controlled in the effectively irreversible nucleophilic attack, but transition state (TS) for this step can be either early or late depending on the nucleophile, ligands, and reaction conditions. In an early TS, the interactions leading to stereochemical differentiation can be understood from the structure of the Pd-allyl intermediate,[13] whereas the late TS is more reminiscent of the Pd-alkene product complex.[14] For the early TS case, stereochemistry is governed by both the population of the Pd-η^3-allyl intermediates and the relative electrophilicity of the allylic carbon atoms. When the TS is late, the formation of the most stable Pd-olefin complex controls enantioselectivity. Previous experience has shown that ammonia can be used as a good model nucleophile,[15] avoiding the problems related to charge separation in conjunction with a continuum solvent model. Note that the use of ammonia as nucleophile instead of dimethyl malonate results in the inversion of the CIP descriptor in the 1,3-diphenylallyl case, due to the change in priority of the groups, although the sense of stereoselectivity is maintained.

We calculated the relative stability of the transition states TS_{endo} and TS_{exo} using NH_3 as nucleophile and the Pd-olefin intermediates (Pd-olefin$_{endo}$ and Pd-olefin$_{exo}$). Only the two *syn*−*syn* allyl complexes were calculated. The contribution of the other allylic species of higher energy (*anti*−*anti* and *syn*−*anti*) was neglected. In this study we have taken into account the configuration of the thioether, the rotation of the thioether substituent, and the attack of the nucleophile *trans* to P and S atoms. In contrast to P,N-ligands, the *trans* effect between the thioether and the phosphite are more similar. Recent studies by Norrby et al. have shown that small changes in sterics can shift the *trans* preference in P,S-ligands.[16] The results of the most stable transition states leading to the formation of both product enantiomers are shown in Table 4 (the results of the full set of calculated TS can be found in the Supporting Information). The energy differences of the calculated TS's using **S1** and **S2** agree with the catalytic results. The energy difference between the TS's using **S1** with ligand **L9f** ($\Delta G^{\#}$ = 18.7 kJ mol^{-1}; ee$_{calc}$ > 99(*S*)) is higher than that of **L9e** ($\Delta G^{\#}$ = 2.9 kJ mol^{-1}; ee$_{calc}$ = 52% (*R*)). This is in good agreement with the higher enantioselectivities achieved using **L9f** (Table 1, > 99% ee for **L9f** vs 33% ee for **L9e**). In addition, the formation of the opposite enantiomers of the substituted product is predicted when **L9e** and **L9f** are used. Similarly, in the reaction of **S2** with

Table 4. Calculated Energies for the Most Stable TS's and Pd−Olefin Complexes Using S1 and S2 and NH_3 as Nucleophile

S1				S2			
Pd-TS		Pd-olefin		Pd-TS		Pd-olefin	
L9e	L9f	L9e	L9f	L9e	L9f	L9e	L9f
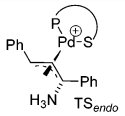	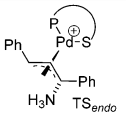	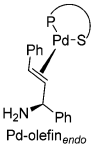	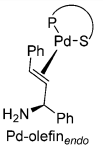	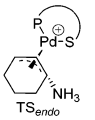	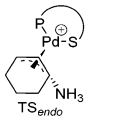	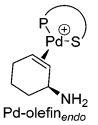	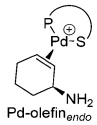
5 kJ/mol	18.7 kJ/mol	0 kJ/mol	14.7 kJ/mol	7.6 kJ/mol	0 kJ/mol	6.8 kJ/mol	0 kJ/mol
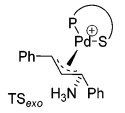	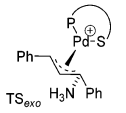	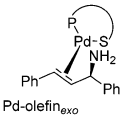	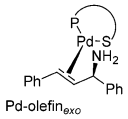	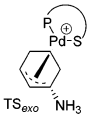	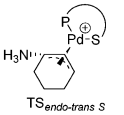	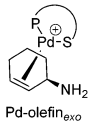	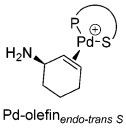
7.9 kJ/mol	0 kJ/mol	10.1 kJ/mol	2.3 kJ/mol	10.3 kJ/mol	4.1 kJ/mol	8.2 kJ/mol	3 kJ/mol

DOI: 10.1021/acs.organomet.6b00547
Organometallics XXXX, XXX, XXX−XXX

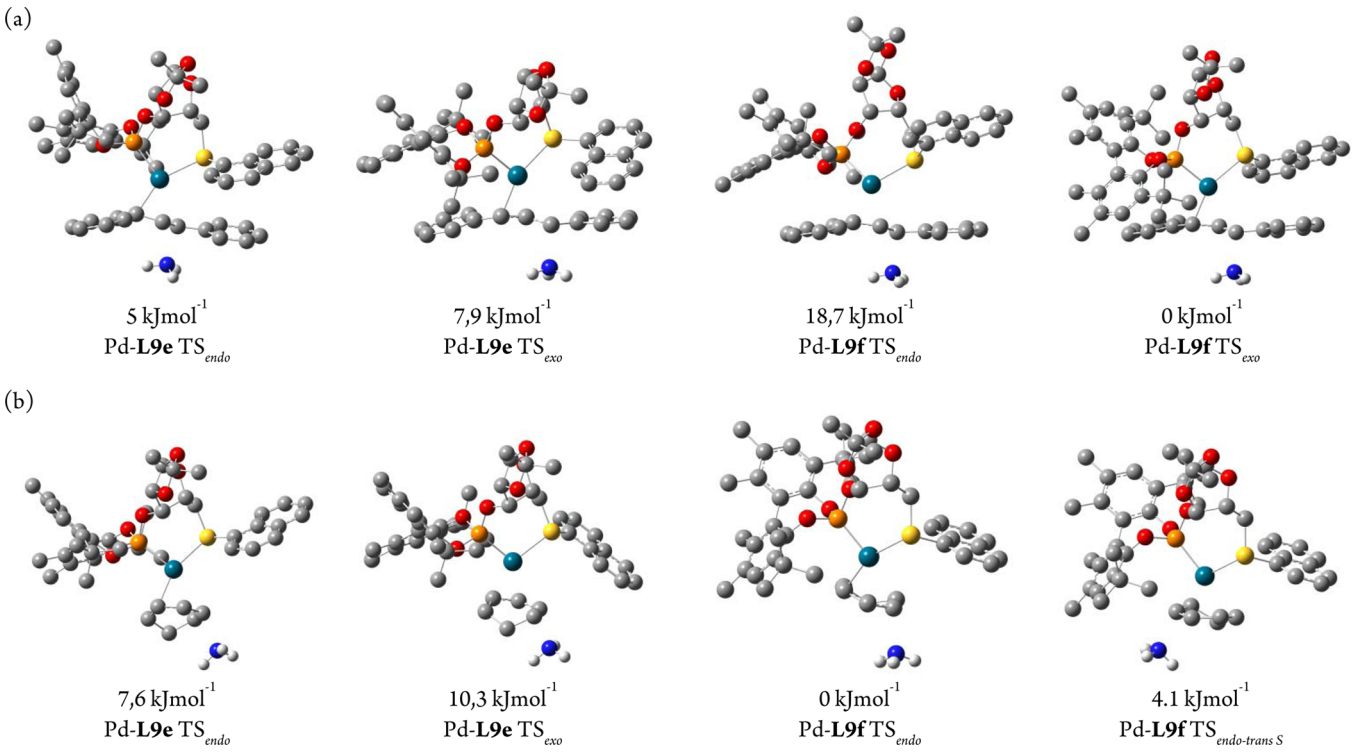

Figure 3. Representation of the calculated most-stable transition states from (a) **S1** and (b) **S2** using ligands **L9e** and **L9f**.

L9f, the TS leading to the product observed experimentally is the most stable one. However, the energy difference between the TS's ($\Delta G^{\#}$ = 4.1 kJ mol^{-1}) is lower than that for substrate **S1** ($\Delta G^{\#}$ = 18.7 kJ mol^{-1}), which agrees with the lower enantioselectivity achieved with **S2**. It should be pointed out that with **S2** and ligand **L9f** both enantiomers of the substitution product arise from TS's with *endo* coordination of the substrate with the nucleophile attack *trans* to P (for the major enantiomer) and *trans* to S (for the minor enantiomer). Figure 3 shows the calculated transition states using ligands **L9e** and **L9f**. We can see that the most stable TS's, which for both substrates contain ligand **L9f** (Pd-**L9f** TS_{exo} for **S1** and Pd-**L9f** TS_{endo} for **S2**), show a different ligand disposition around the metal center than the less stable TS's. As a consequence, the biaryl phosphite moiety in ligand **L9f** has the sufficient flexibility to generate a suitable chiral pocket that can effectively accommodate both types of substrates, thereby yielding high enantioselectivities for both substrates.

However, the calculated energies of the Pd-olefin intermediates do not correlate well with the experimental results. For instance, although the calculated results of the Pd-olefin complexes of **S1** correctly predict the formation of opposite enantiomers of the substitution products with **L9e** and **L9f**; the calculated energy differences between both Pd-olefin complexes are very similar for both ligands (for ligand **L9e**, $\Delta G^{\#}$ = 10.1 kJ mol^{-1}; ee_{calc} = 97% (*R*); for ligand **L9f**, $\Delta G^{\#}$ = 12.3 kJ mol^{-1}; ee_{calc} = 99% (*S*)). This indicates that if the reaction proceeds via a late TS then both ligands should provide similar levels of enantioselectivity which does not agree with the experimental results.

Preparation and NMR Study of Pd-Allyl Intermediates. DFT studies have shown that enantioselectivity is determined during the nucleophilic attack. Consequently, the structural elucidation of the Pd-allyl intermediates and the determination of their relative reactivity toward the nucleophile are crucial to understand their catalytic behavior. For this purpose, we next studied the Pd-π-allyl compounds **39**–**43** [Pd(η^3-allyl)(L)]BF_4 (L = **L1a**, **L9e**,**f** and **L13e**). Pd-complexes **39**–**43** containing 1,3-diphenyl, 1,3-dimethyl, or cyclohexenyl allyl groups were prepared as previously reported from the corresponding Pd-allyl dimer and the appropriate ligand in the presence of silver tetrafluoroborate (Scheme 1).[17] We have used ^{1}H, ^{13}C, and ^{31}P

Scheme 1. Preparation of [Pd(η^3-allyl)(L)]BF_4 Complexes 39–43

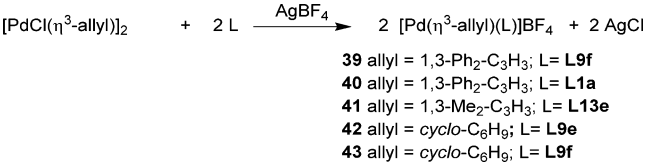

NMR spectroscopy to characterize them. The NMR assignments have been performed using the information from ^{1}H–^{1}H, ^{31}P–^{1}H, and ^{13}C–^{1}H correlation measurements in combination with ^{1}H–^{1}H NOESY experiments. Unfortunately, we were unable to achieve crystal of sufficient quality to make X-ray diffraction measurements.

The VT-NMR study (30 °C to −80 °C) of Pd-1,3-diphenyl allyl intermediate **39**, which contains the ligand that has provided the highest enantioselectivity in the allylic substitution of **S1** (Table 1), showed a 1:4 mixture of two isomers in equilibrium (Scheme 2).

Both isomers were unambiguously assigned by NMR to the two *syn*/*syn* Pd-η^3-*endo* and *exo* isomers. In both isomers, the NOE indicated interactions between the two terminal protons of the allyl group, which clearly indicates a *syn*/*syn* disposition. In addition, for the major isomer, one of the *tert*-butyl substituents of the phosphite moiety (the one that shows NOE interaction with the hydrogen attached to C3) showed NOE-

DOI: 10.1021/acs.organomet.6b00547
Organometallics XXXX, XXX, XXX–XXX

Scheme 2. Diastereoisomer Pd-allyl Intermediates for S1 with Ligand L9f (Isomers 39)[a]

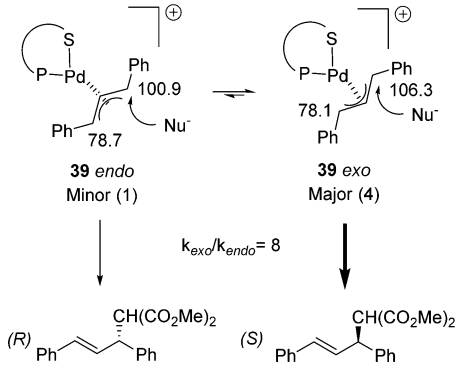

[a]The relative amounts of each isomer are shown in parentheses. The chemical shifts (in ppm) of the allylic terminal carbons are also shown.

interaction with the terminal allyl proton *trans* to the thioether group, while for the minor isomer this interaction appears with the central allyl proton (Figure 4). These interactions can be

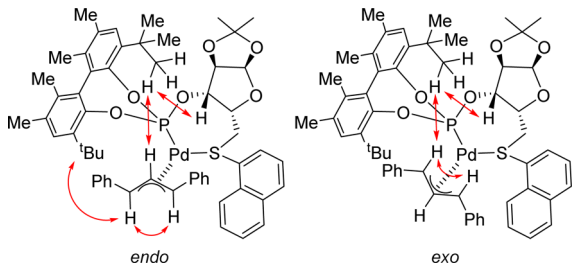

Figure 4. Main NOE contacts for Pd-allyl intermediates **39**.

explained by assuming a *syn*/*syn* Pd-*exo* disposition for the major isomer and an *endo* disposition for the minor isomer. Although the population of the Pd-allyl intermediates obtained by DFT calculations is different than those found by NMR, the general trend is reproduced well (see Table S1). Thus, the major isomer is Pd-η^3-*exo*. The carbon chemical shifts of compound **39** indicate that the most electrophilic allylic terminal carbon is located *trans* to the phosphite moiety in the major isomer ($\Delta\delta(^{13}C) \approx 5.4$ ppm). Assuming that the nucleophilic attack takes place at the more electrophilic allyl carbon terminus and in line with the DFT calculations, the stereochemical outcome of the reaction is not fully controlled by the population of the Pd-allyl intermediates (note that the diastereomeric excesses differ from the enantiomeric excesses), so the relative electrophilicity of the terminal allylic carbons of each isomer plays an important role and has to be taken into account. The excellent enantioselectivities obtained with Pd-**9f** catalytic system can be therefore explained by the fact that the major isomer is also the fast-reacting one. To prove this, we studied the reactivity of Pd-1,3-diphenyl allyl intermediate **39** with sodium malonate at low temperature (−80 °C) by *in situ* NMR (see Supporting Information). Our results showed that the major *exo* isomer reacts around 8 times faster than the *endo* isomer, affording the alkylation product in 96% (*S*) ee. If we take into account the relative reaction rates and the abundance of both isomers, then the calculated ee should be 94% (*S*), which is in a good accordance with the ee obtained experimentally.

We also studied Pd-1,3-diphenyl allyl intermediate **40**. This contains ligand **L1a** which differs from previous ligand **L9f** in the presence of an achiral biaryl phosphite moiety and provided low enantioselectivity in the substitution of **S1** (Table 1). As for intermediate **39**, a 1:4 mixture of two isomers in equilibrium was observed (Scheme 3). However, an important difference is

Scheme 3. Diastereoisomer Pd-allyl Intermediates for S1 with Ligands L1a (Isomers 40)[a]

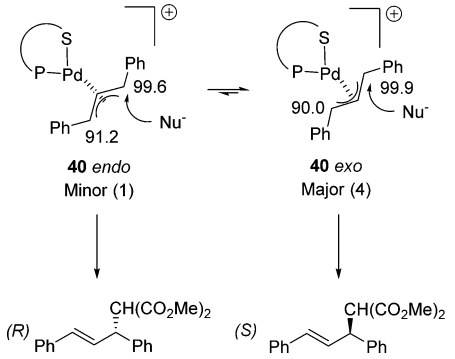

[a]The relative amounts of each isomer are shown in parentheses. The chemical shifts (in ppm) of the allylic terminal carbons are also shown.

that the electrophilicities of the allylic terminal carbon atom *trans* to the phosphite are rather similar in both complexes ($\Delta\delta(^{13}C) \approx 0.3$ ppm), which makes both species react at similar rate. This agrees with the low enantioselectivity obtained with Pd-**L1a**.

We next studied Pd π-allyl complex [Pd(η^3-1,3-dimethyl-allyl)(**L13e**)]BF_4 (**41**) with unhindered linear substrate **S3** and the ligand that had provided the highest enantioselectivity. The VT-NMR study (30 °C to −80 °C) showed a 1:3 mixture of two isomers in equilibrium, which were assigned by NMR to the two *syn*/*syn* Pd-η^3-*endo* and *exo* isomers (Scheme 4). In

Scheme 4. Diastereoisomer Pd-allyl Intermediates for S3 with Ligands L13e (Isomers 41)[a]

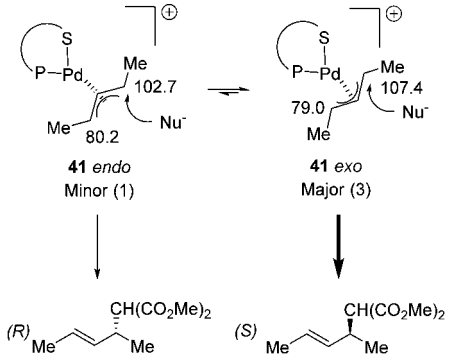

[a]The relative amounts of each isomer are shown in parentheses. The chemical shifts (in ppm) of the allylic terminal carbons are also shown.

both isomers, the NOE indicated interactions between the central allyl proton and the two methyl substituents, which clearly indicates a *syn*/*syn* disposition. In addition, for the minor *endo* isomer, there is a NOE interaction between the central allyl proton and the *tert*-butyl substituent of the phosphite moiety that shows NOE with the hydrogen attached to C4 (Figure 5). For the major *exo* isomer, there is a NOE interaction between one of the methyl substituents of the

DOI: 10.1021/acs.organomet.6b00547
Organometallics XXXX, XXX, XXX−XXX

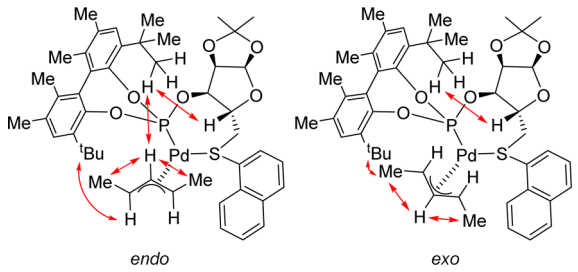

Figure 5. Main NOE contacts for Pd-allyl intermediates **41**.

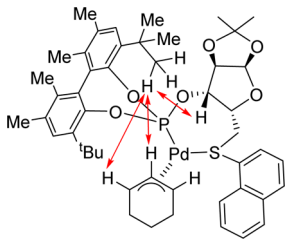

Figure 6. Main NOE contacts for the major isomer of Pd-allyl intermediates **42** and **43**.

substrate (the one *trans* to the thioether) and one of the *tert*-butyl substituents of the phosphite group (the one that does not show NOE with the hydrogen attached to C4 of the furanoside backbone; Figure 5). The carbon chemical shifts show that the most electrophilic allylic terminal carbon is located *trans* to the phosphite in the major isomer ($\Delta\delta(^{13}C) \approx 4.7$ ppm). The high enantioselectivity obtained with Pd/**L13e** system can be therefore attributed to the fact that the major isomer is also the fastest-reacting one.

Finally, in an attempt to learn more how the configuration of the biaryl phosphite group affects the enantioselectivity observed in the allylic substitution of the unhindered cyclic substrate **S3**, we studied Pd-1,3-cyclohexenyl-allyl intermediate **42**, which contains **L9e**, and compared it with its related counterpart Pd/**L9f** (compound **43**). The VT-NMR study (30 °C to −80 °C) of Pd-1,3-cyclohexenyl allyl intermediates **42** and **43** showed a mixture of two isomers in equilibrium at a ratio of 3:2 and >20:1, respectively (Scheme 5). The major isomers were unambiguously assigned by NOE to Pd-η^3-*endo* isomers. Thus, NOE interactions were found between one of the *tert*-butyl substituents of the phosphite moiety (the one that shows NOE interaction with the hydrogen attached to C3) and the central allyl proton and the allyl proton *trans* to the thioether group (Figure 6). The same population of the Pd-allyl intermediates was predicted by DFT (see Table S1). The carbon NMR chemical shifts indicated that the most electrophilic allylic terminus carbon is *trans* to the phosphite moiety. For complex **42**, the fact that the electrophilicity of the allylic terminal carbon atom *trans* to the phosphite is rather similar in both complexes ($\Delta\delta(^{13}C) \approx 1.1$ ppm) suggests that both isomers react at a similar rate, so the enantioselectivity is mainly affected by the population of the *endo* and *exo* isomers. The much higher enantioselectivity obtained using Pd-**L9f** can therefore be attributed to the fact that only one Pd-allyl intermediate is detected.

CONCLUSIONS

A large library of furanoside phosphite/phosphinite/phosphine-thioether ligands **L1**−**L17a**−**l** has been applied in the Pd-catalyzed allylic substitution of several substrates using a wide range of nucleophiles. These ligands, which are prepared from inexpensive D-xylose, have the advantages of the robustness of the thioether moiety and the extra control provided by the flexibility of the chiral pocket through the presence of a biaryl phosphite group and a modular sugar backbone. Other advantages are that they are stable to air and other oxidizing agents and can be manipulated/stored in air. The structural variety of this library allowed us to investigate the effect on catalytic performance of systematically varying the position of the thioether group at either C5 or C3 of the furanoside backbone and the effect of the configuration at C3 of the furanoside backbone. We also studied the effects of the substituents in the thioether group, the configuration of the biaryl phosphite moiety and of their substituents, and the replacement of the phosphite moiety by either a phosphinite group or a phosphine group. By choosing the ligand components, we have identified catalytic systems that create C−C, C−N, and C−O bonds in hindered and unhindered substrates for a wide range of nucleophiles in high enantioselectivities (ee's up to >99%) and yields. We note the excellent enantioselectivities achieved in the etherification of linear and cyclic substrates, which represent the first successful etherification of both hindered and unhindered substrates. The results presented here compete very well with a few other ligands that also provide high ee in several substrate types using C-, N-, and O-nucleophiles. Moreover, the process

Scheme 5. Diastereoisomer Pd-allyl Intermediates for S2 with Ligands L9e (Isomers 42) and L9f (Isomer 43)[a]

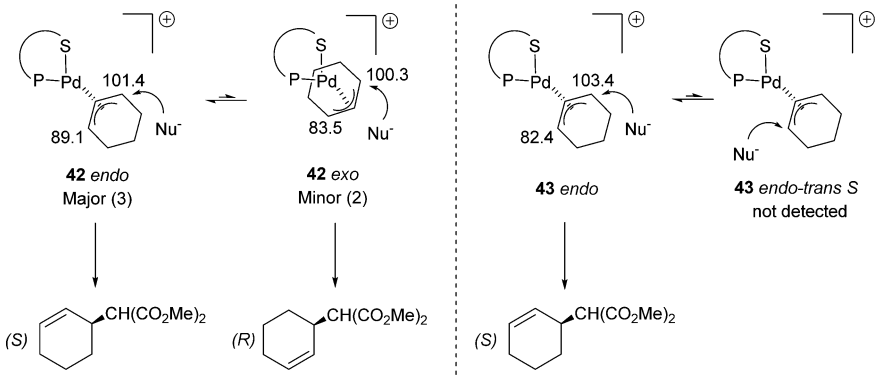

[a]The relative amounts of each isomer are shown in parentheses. The chemical shifts (in ppm) of the allylic terminal carbons are also shown.

DOI: 10.1021/acs.organomet.6b00547
Organometallics XXXX, XXX, XXX−XXX

can be carried out in propylene carbonate as alternative environmentally friendly solvent with no loss of enantioselectivity. A DFT computational study of the key intermediates and transition states involved in the enantiocontrol is in agreement with an early transition state. Further studies on the Pd π-allyl intermediates improved our understanding of the effect of the ligand parameters on the origin of the enantioselectivity. Therefore, for enantioselectivities to be high, the ligand parameters need to be correctly combined so that either the Pd-intermediate that has the fastest reaction with the nucleophile is predominantly formed (for linear hindered **S1** and unhindered **S3** type substrates) and/or that one of the isomers is predominantly formed (for unhindered cyclic **S2**). These results open up the enantioselective Pd-allylic substitution of several substrate types with a large variety of nucleophiles to the potential effective use of readily available, easy to handle, and highly modular phosphite-thioether ligands.

EXPERIMENTAL SECTION

General Considerations. All reactions were carried out using standard Schlenk techniques under an argon atmosphere. Commercial chemicals were used as received. Solvents were dried by means of standard procedures and stored under argon. ^{1}H, ^{13}C{^{1}H}, and ^{31}P{^{1}H} NMR spectra were recorded using a Varian Mercury 400 MHz spectrometer. Chemical shifts are relative to that of $SiMe_4$ (^{1}H and ^{13}C{^{1}H}) as an internal standard. Racemic substrates **S1**−**S10** were prepared as previously reported.[18] Ligands **L1**−**L17a**−**l** were prepared as previously described.[19]

Computational Details. Geometries of all transition states and intermediates were optimized using the Gaussian 09 program,[20] employing the B3LYP[21] density functional and the LANL2DZ[22] basis set for palladium and the 6-31G*[23] basis set for all other elements. Solvation correction was applied in the course of the optimizations using the PCM model with the default parameters for dichloromethane.[24] The complexes were treated with charge +1 and in the singlet state. No symmetry constraints were applied. Normal mode analysis of all transition states revealed a single imaginary mode corresponding to the expected nucleophilic attack of ammonia to one of the two allylic termini. The energies were further refined by performing single-point calculations using the above-mentioned parameters, with the exception that the 6-311+G**[25] basis set was used for all elements except for palladium, and by applying dispersion correction using the DFT-D3[26] model. All energies reported are Gibbs free energies at 298.15 K and calculated as $G_{reported} = G_{6\text{-}31G^*} + E_{6\text{-}311+G^{**}} - E_{6\text{-}31G^*} + E_{DFT\text{-}D3}$.

Typical Procedure for the Allylic Alkylation. A degassed solution of $[PdCl(\eta^3\text{-}C_3H_5)]_2$ (1.8 mg, 0.005 mmol) and the corresponding ligand (0.011 mmol) in dichloromethane (0.5 mL) was stirred for 30 min. Subsequently, a solution of the corresponding substrate (1 mmol) in dichloromethane (1.5 mL), nucleophile (3 mmol), *N*,*O*-bis(trimethylsilyl)-acetamide (740 μL, 3 mmol), and the corresponding base (5 mol %) were added. The reaction mixture was stirred at room temperature. After the desired reaction time, the reaction mixture was diluted with Et_2O (5 mL), and saturated NH_4Cl (aq) (25 mL) was added. The mixture was extracted with Et_2O (3 × 10 mL) and the extract dried over $MgSO_4$. For compounds **1**, **4**−**26**, **29**, **30**, **33**, and **34**, the solvent was removed, conversions were measured by ^{1}H NMR, and enantiomeric excesses were determined by HPLC. For compounds **2**, **3**, **27**, **31**, **32** and **36**−**38**, conversion and enantiomeric excesses were determined by GC. For compounds **28** and **35**, conversion were measured by ^{1}H NMR, and ee's were determined by ^{1}H NMR using $[Eu(hfc)_3]$.

Typical Procedure for the Allylic Amination. A degassed solution of $[PdCl(\eta^3\text{-}C_3H_5)]_2$ (1.8 mg, 0.005 mmol) and the corresponding ligand (0.011 mmol) in dichloromethane (0.5 mL) was stirred for 30 min. Subsequently, a solution of the corresponding substrate (1 mmol) in dichloromethane (1.5 mL) and benzylamine (262 μL, 3 mmol) was added. The reaction mixture was stirred at room temperature. After the desired reaction time, the reaction mixture was diluted with Et_2O (5 mL), and saturated NH_4Cl (aq) (25 mL) was added. The mixture was extracted with Et_2O (3 × 10 mL) and the extract dried over $MgSO_4$. The solvent was removed, conversions were measured by ^{1}H NMR, and enantiomeric excesses of compounds were determined by HPLC.

Typical Procedure for the Allylic Etherification. A degassed solution of $[PdCl(\eta^3\text{-}C_3H_5)]_2$ (0.9 mg, 0.0025 mmol) and the corresponding ligand (0.0055 mmol) in dichloromethane (0.5 mL) was stirred for 30 min. Subsequently, a solution of the corresponding substrate (31.5 mg, 0.125 mmol) in dichloromethane (1.5 mL) was added. After 10 min, Cs_2CO_3 (122 mg, 0.375 mmol) and benzyl alcohol (40 μL, 0.375 mmol) were added. The reaction mixture was stirred at room temperature. After the desired reaction time, the reaction mixture was diluted with Et_2O (5 mL), and saturated NH_4Cl (aq) (25 mL) was added. The mixture was extracted with Et_2O (3 × 10 mL) and the extract dried over $MgSO_4$. The solvent was removed, conversions were measured by ^{1}H NMR, and enantiomeric excesses were determined by HPLC.

Preparation of Pd-Allyl Intermediates. The corresponding ligand (0.05 mmol) and the complex [Pd(μ-Cl)(η^3-1,3-allyl)]2 (0.025 mmol) were dissolved in CD2Cl2 (1.5 mL) at room temperature under argon. AgBF4 (9.8 mg, 0.05 mmol) was added after 30 min and the mixture was stirred for 30 min. The mixture was then filtered over Celite under argon and the resulting solutions were analyzed by NMR. After the NMR analysis, the complexes were precipitated as pale yellow solids by adding hexane.

*[Pd(η^3-1,3-diphenylallyl)(**L9f**)]BF_4 (**39**).* Isomer *endo* (20%): ^{31}P NMR (161 MHz, CD_2Cl_2, δ) 137.1 (s). ^{1}H NMR (400 MHz, CD_2Cl_2, δ) 1.19 (s, 3H, CH_3), 1.32 (s, 3H, CH_3), 1.58 (s, 9H, CH_3, *t*-Bu), 1.67 (s, 9H, CH_3, *t*-Bu), 1.72 (s, 3H, CH_3), 1.76 (s, 3H, CH_3), 2.31 (s, 3H, CH_3), 2.37 (s, 3H, CH_3), 3.21 (m, 1H, H5′), 3.56 (dd, 1H, H5, $^{2}J_{5-5'}$ = 12.4 Hz, $^{3}J_{5-4}$ = 4.8 Hz), 4.42 (m, 2H, H4, CH═allyl *trans* to S), 4.63 (d, 1H, H2, $^{3}J_{2-1}$ = 3.6 Hz), 4.97 (b, 1H, H3), 5.03 (m, 1H, CH═allyl *trans* to P), 5.71 (d, 1H, H1, $^{3}J_{1-2}$ = 3.6 Hz), 6.42 (m, 1H, CH═allyl central), 6.5−8.4 (m, 17H, CH═). ^{13}C NMR (100 MHz, CD_2Cl_2, δ) 16.8 (CH_3), 17.1 (CH_3), 20.6 (CH_3), 20.7 (CH_3), 26.4 (CH_3), 27.0 (CH_3), 32.2 (CH_3, *t*-Bu), 32.3 (CH_3, *t*-Bu), 35.2 (C, *t*-Bu), 35.7 (C, *t*-Bu), 41.8 (C5), 77.0 (C4), 78.7 (b, CH═allyl *trans* to S), 81.7 (b, C3), 84.4 (C2), 100.9 (d, CH═allyl *trans* to P, J_{C-P} = 33.2 Hz), 105.5 (C1), 112.2 (d, CH═allyl central, J_{C-P} = 9.2 Hz), 113.5 (CMe_2), 124.1−143.9 (aromatic carbons). Isomer *exo* (80%): ^{31}P NMR (161 MHz, CD_2Cl_2, δ) 138.0 (s). ^{1}H NMR (400 MHz, CD_2Cl_2, δ) 1.22 (s, 3H, CH_3), 1.36 (s, 3H, CH_3), 1.38 (s, 9H, CH_3, *t*-Bu), 1.74 (s, 3H, CH_3), 1.78 (s, 3H, CH_3), 1.81 (s, 9H, CH_3, *t*-Bu), 2.25 (s, 3H, CH_3), 2.47 (s, 3H, CH_3), 3.39 (m, 2H, H5′, H5), 4.21 (d, 1H, H2, $^{3}J_{2-1}$ = 3.6 Hz), 4.32 (m, 1H, H4), 4.97 (m, 1H, CH═allyl *trans* to S), 5.00 (b, 1H, H3), 5.52 (m, 1H, CH═allyl *trans* to P), 5.64 (d, 1H, H1, $^{3}J_{1-2}$ = 3.6 Hz), 6.24 (m, 1H, CH═allyl central), 6.5−8.4 (m, 17H, CH═). ^{13}C NMR (100 MHz, CD_2Cl_2, δ) 16.9 (CH_3), 17.3 (CH_3), 20.6 (CH_3), 20.8 (CH_3), 26.5 (CH_3), 26.8 (CH_3), 32.0 (CH_3, *t*-Bu), 32.7 (CH_3, *t*-Bu), 35.2 (C, *t*-Bu), 35.8 (C, *t*-Bu), 39.6 (C5), 76.4 (C4), 78.1 (b, CH═allyl *trans* to S), 81.7 (b, C3), 84.6 (C2), 105.1 (C1), 106.3 (d, CH═allyl *trans* to P, J_{C-P} = 32.4 Hz), 110.9 (d, CH═allyl central, J_{C-P} = 9.5 Hz), 113.3 (CMe_2), 124.1−143.9 (aromatic carbons). MS HR-ESI [found 1013.3187, $C_{57}H_{64}O_6PPdS$ $(M - BF_4)^+$ requires 1013.3191].

*[Pd(η^3-1,3-diphenylallyl)(**L1a**)]BF_4 (**40**).* Isomer *exo* (80%): ^{31}P NMR (161 MHz, CD_2Cl_2, δ) 143.6 (s). ^{1}H NMR (400 MHz, CD_2Cl_2, δ) 1.25 (s, 3H, CH_3), 1.28 (s, 3H, CH_3), 1.36 (s, 9H, CH_3, *t*-Bu), 1.45 (s, 9H, CH_3, *t*-Bu), 1.59 (s, 9H, CH_3, *t*-Bu), 1.63 (s, 9H, CH_3, *t*-Bu), 3.00 (dd, 1H, H5′, $^{2}J_{5'-5}$ = 13.6 Hz, $^{3}J_{5'-4}$ = 11.6 Hz), 3.56 (dd, 1H, H5, $^{2}J_{5-5'}$ = 13.6 Hz, $^{3}J_{5-4}$ = 4.0 Hz), 4.09 (m, 1H, H4), 4.53 (d, 1H, H2, $^{3}J_{2-1}$ = 4.0 Hz), 5.66 (m, 2H, H3, CH═allyl *trans* to S), 5.73 (d, 1H, H1, $^{3}J_{1-2}$ = 4.0 Hz), 5.83 (m, 1H, CH═allyl *trans* to P), 6.56 (m, 1H, CH═allyl central), 6.7−7.7 (m, 19H, CH═). ^{13}C NMR (100 MHz, CD_2Cl_2, δ) 26.5 (CH_3), 26.6 (CH_3), 31.6 (CH_3, *t*-Bu), 31.7 (CH_3, *t*-Bu), 32.0 (CH_3, *t*-Bu), 32.3 (CH_3, *t*-Bu), 35.1 (C, *t*-Bu), 35.2 (C, *t*-Bu), 35.8 (C, *t*-Bu), 36.5 (C, *t*-Bu), 37.3 (b, C5), 76.2 (C4), 78.8

DOI: 10.1021/acs.organomet.6b00547
Organometallics XXXX, XXX, XXX−XXX

(d, C3, J_{C-P} = 10.7 Hz), 85.1 (d, C2, J_{C-P} = 8.4 Hz), 90.0 (b, CH═ allyl *trans* to S), 99.9 (d, CH═allyl *trans* to P, J_{C-P} = 32.4 Hz), 104.9 (C1), 113.0 (CMe_2), 114.4 (d, CH═allyl central, J_{C-P} = 10.1 Hz), 125.4−149.4 (aromatic carbons). Isomer *endo* (20%): ^{31}P NMR (161 MHz, CD_2Cl_2, δ) 140.6 (s). ^{1}H NMR (400 MHz, CD_2Cl_2, δ) 1.15 (s, 3H, CH_3), 1.18 (s, 3H, CH_3), 1.37 (s, 9H, CH_3, *t*-Bu), 1.47 (s, 9H, CH_3, *t*-Bu), 1.59 (s, 9H, CH_3, *t*-Bu), 1.72 (s, 9H, CH_3, *t*-Bu), 3.29 (m, 1H, H5′), 3.64 (dd, 1H, H5, $^2J_{5-5'}$ = 13.6 Hz, $^3J_{5-4}$ = 4.8 Hz), 3.92 (m, 1H, H4), 4.28 (d, 1H, H2, $^3J_{2-1}$ = 3.6 Hz), 4.92 (m, 1H, H3), 5.30 (m, 1H, CH═allyl *trans* to S), 5.44 (m, 1H, CH═allyl *trans* to P), 5.71 (d, 1H, H1, $^3J_{1-2}$ = 3.6 Hz), 6.81 (m, 1H, CH═allyl central), 6.7−7.7 (m, 19H, CH═). ^{13}C NMR (100 MHz, CD_2Cl_2, δ) 26.2 (CH_3), 26.4 (CH_3), 31.6 (CH_3, *t*-Bu), 31.7 (CH_3, *t*-Bu), 32.0 (CH_3, *t*-Bu), 32.3 (CH_3, *t*-Bu), 35.2 (C, *t*-Bu), 35.3 (C, *t*-Bu), 35.8 (C, *t*-Bu), 36.2 (C, *t*-Bu), 38.1 (b, C5), 76.2 (C4), 78.8 (d, C3, J_{C-P} = 10.7 Hz), 84.6 (d, C2, J_{C-P} = 7.8 Hz), 91.2 (b, CH═allyl *trans* to S), 99.6 (d, CH═allyl *trans* to P, J_{C-P} = 33.4 Hz), 104.9 (C1), 109.8 (d, CH═allyl central, J_{C-P} = 9.8 Hz), 113.0 (CMe_2), 125.4−149.4 (aromatic carbons). MS HR-ESI [found 1019.3656, $C_{57}H_{70}O_6PPdS$ $(M - BF_4)^+$ requires 1019.3660].

*[Pd(η^3-1,3-dimethylallyl)(**L13e**)]BF_4 (**41**).* Isomer *endo* (25%): ^{31}P NMR (161 MHz, CD_2Cl_2, δ) 137.4 (s). ^{1}H NMR (400 MHz, CD_2Cl_2, δ) 0.59 (d, 3H, CH_3, $^3J_{H-H}$ = 5.6 Hz), 1.14 (d, 3H, CH_3, $^3J_{H-H}$ = 6.0 Hz), 1.16 (s, 3H, CH_3), 1.31 (s, 3H, CH_3), 1.44 (s, 9H, CH_3, *t*-Bu), 1.55 (s, 9H, CH_3, *t*-Bu), 1.78 (s, 3H, CH_3), 1.85 (s, 3H, CH_3), 2.29 (s, 3H, CH_3), 2.34 (s, 3H, CH_3), 3.41 (m, 1H, CH═ *trans* to S), 3.46 (m, 1H, H5), 3.58 (m, 1H, CH═ *trans* to P), 3.91 (m, 1H, H5′), 4.48 (m, 1H, H3), 4.54 (m, 1H, H2), 4.86 (m, 1H, H4), 5.00 (m, 1H, CH═ central), 5.75 (d, 1H, H1, $^3J_{1-2}$ = 4.0 Hz), 7.1−8.6 (m, 9H, CH═). ^{13}C NMR (100 MHz, CD_2Cl_2, δ) 16.2−17.1 (CH_3 allyl), 16.7 (b, CH_3), 20.3 (CH_3), 26.0 (CH_3), 26.1 (CH_3), 31.0−31.9 (CH_3, *t*-Bu), 34.9−35.2 (C, *t*-Bu), 37.6 (C5), 75.9−76.5 (C4, C3), 80.2 (b, CH═ *trans* to S), 83.7 (C2), 102.7 (d, CH═*trans* to P, J_{C-P} = 35.2 Hz), 104.5 (C1), 112.8 (CMe_2), 116.5 (d, CH═ central, J_{C-P} = 12.1 Hz), 122−146 (aromatic carbons). Isomer *exo* (75%): ^{31}P NMR (161 MHz, CD_2Cl_2, δ) 138.2 (s). ^{1}H NMR (400 MHz, CD_2Cl_2, δ) 0.77 (d, 3H, CH_3, $^3J_{H-H}$ = 6.4 Hz), 0.92 (d, 3H, CH_3, $^3J_{H-H}$ = 6.4 Hz), 1.21 (s, 3H, CH_3), 1.39 (s, 9H, CH_3, *t*-Bu), 1.44 (s, 3H, CH_3), 1.52 (s, 9H, CH_3, *t*-Bu), 1.74 (s, 3H, CH_3), 1.92 (s, 3H, CH_3), 2.26 (s, 3H, CH_3), 2.27 (s, 3H, CH_3), 3.32 (m, 1H, CH═ *trans* to S), 3.46 (m, 1H, H5), 3.5 (m, 1H, CH═ *trans* to P), 3.99 (m, 1H, H5′), 4.58 (m, 1H, H3), 4.72 (m, 1H, H2), 4.86 (m, 1H, H4), 4.93 (m, 1H, CH═ central), 5.78 (d, 1H, H1, $^3J_{1-2}$ = 4.0 Hz), 7.1−8.6 (m, 9H, CH═). ^{13}C NMR (100 MHz, CD_2Cl_2, δ) 16.2−17.1 (CH_3 allyl), 16.7 (b, CH_3), 20.4 (CH_3), 20.6 (CH_3), 26.1 (CH_3), 26.2 (CH_3), 31.0−31.9 (CH_3, *t*-Bu), 34.9−35.2 (C, *t*-Bu), 39.2 (C5), 75.9−76.5 (C4, C3), 79.0 (b, CH═ *trans* to S), 83.6 (C2), 104.5 (C1), 107.4 (d, CH═*trans* to P, J_{C-P} = 36.6 Hz), 113.1 (CMe_2), 116.8 (d, CH═ central, J_{C-P} = 10.9 Hz), 122−146 (aromatic carbons). MS HR-ESI [found 867.3028, $C_{45}H_{62}O_6PPdS$ $(M - BF_4)^+$ requires 867.3034].

*[Pd(η^3-1,3-cyclohexenylallyl)(**L9e**)]BF_4 (**42**).* Isomer *endo* (60%): ^{31}P NMR (161 MHz, CD_2Cl_2, δ) 139.5 (s). ^{1}H NMR (400 MHz, CD_2Cl_2, δ) 0.87−1.09 (m, 2H, CH_2), 1.20 (s, 3H, CH_3), 1.28−1.40 (m, 2H, CH_2), 1.32 (s, 3H, CH_3), 1.53 (s, 9H, CH_3, *t*-Bu), 1.62 (s, 9H, CH_3, *t*-Bu), 1.80−2.10 (m, 2H, CH_2), 1.83 (s, 3H, CH_3), 1.86 (s, 3H, CH_3), 2.32 (s, 3H, CH_3), 2.33 (s, 3H, CH_3), 3.21 (m, 1H, H4), 3.77 (m, 1H, H5′), 3.93 (m, 1H, H5), 4.46 (d, 1H, H2, $^3J_{2-1}$ = 3.6 Hz), 4.69 (m, 1H, CH═allyl *trans* to S), 5.13 (dd, 1H, H3, $^3J_{3-P}$ = 13.2 Hz, $^3J_{3-4}$ = 2.0 Hz), 5.72 (d, 1H, H1, $^3J_{1-2}$ = 3.6 Hz), 5.93 ((m, 1H, CH═ allyl *trans* to P), 6.17 (m, 1H, CH═allyl central), 7.29 (d, 1H, CH═, *J* = 6 Hz), 7.6−7.8 (m, 4H, CH═), 8.0−8.2 (m, 2H, CH═), 8.50 (d, 1H, CH═, *J* = 8.4 Hz). ^{13}C NMR (100 MHz, CD_2Cl_2, δ) 16.3 (CH_3), 16.4 (CH_3), 19.3 (CH_2), 20.0 (CH_3), 20.1 (CH_3), 25.8 (CH_3), 25.9 (CH_3), 28.1 (CH_2), 29.0 (CH_2), 31.3 (CH_3, *t*-Bu), 31.4 (CH_3, *t*-Bu), 34.7 (C, *t*-Bu), 35.0 (C, *t*-Bu), 38.5 (b, C5), 75.8 (C4), 78.2 (d, C3, J_{C-P} = 10.7 Hz), 84.2 (d, C2, J_{C-P} = 9.1 Hz), 89.1 (d, CH═allyl *trans* to S, J_{C-P} = 6.8 Hz), 101.4 (d, CH═allyl *trans* to P, J_{C-P} = 34.2 Hz), 104.1 (C1), 112.4 (CMe_2), 114.6 (d, CH═allyl central, J_{C-P} = 9.9 Hz), 123.5−144.9 (aromatic carbons). Isomer *exo* (40%): ^{31}P NMR (161 MHz, CD_2Cl_2, δ) 139.2 (s). ^{1}H NMR (400 MHz, CD_2Cl_2, δ) 0.87−1.09 (m, 2H, CH_2), 1.11 (s, 3H, CH_3), 1.28−1.40 (m, 2H, CH_2), 1.28 (s, 3H, CH_3), 1.50 (s, 9H, CH_3, *t*-Bu), 1.54 (s, 9H, CH_3, *t*-Bu), 1.80−2.10 (m, 2H, CH_2), 1.85 (s, 3H, CH_3), 1.99 (s, 3H, CH_3), 2.33 (s, 3H, CH_3), 2.34 (s, 3H, CH_3), 3.62 (m, 1H, H4), 3.77 (m, 1H, H5′), 3.93 (m, 1H, H5), 4.55 (d, 1H, H2, $^3J_{2-1}$ = 3.6 Hz), 4.61 (m, 1H, CH═allyl *trans* to S), 5.24 (m, 2H, H3, CH═allyl *trans* to P), 5.87 (d, 1H, H1, $^3J_{1-2}$ = 3.6 Hz), 5.95 (m, 1H, CH═allyl central), 7.31 (d, 1H, CH═, *J* = 6 Hz), 7.6−7.8 (m, 4H, CH═), 8.0−8.2 (m, 2H, CH═), 8.38 (d, 1H, CH═, *J* = 8.4 Hz). ^{13}C NMR (100 MHz, CD_2Cl_2, δ) 16.0 (CH_3), 16.8 (CH_3), 19.3 (CH_2), 20.0 (CH_3), 20.1 (CH_3), 25.7 (CH_3), 26.1 (CH_3), 29.3 (b, CH_2), 29.6 (CH_2), 31.7 (CH_3, *t*-Bu), 32.2 (CH_3, *t*-Bu), 34.9 (C, *t*-Bu), 35.2 (C, *t*-Bu), 38.5 (b, C5), 76.4 (C4), 78.0 (d, C3, J_{C-P} = 7.5 Hz), 83.5 (d, CH═allyl *trans* to S, J_{C-P} = 6.9 Hz), 84.5 (d, C2, J_{C-P} = 7.6 Hz), 100.3 (d, CH═allyl *trans* to P, J_{C-P} = 34.0 Hz), 104.2 (C1), 112.8 (CMe_2), 113.6 (d, CH═allyl central, J_{C-P} = 9.9 Hz), 123.5−144.9 (aromatic carbons). MS HR-ESI [found 901.2872, $C_{48}H_{60}O_6PPdS$ $(M - BF_4)^+$ requires 901.2878].

*[Pd(η^3-1,3-cyclohexenylallyl)(**L9f**)]BF_4 (**43**).* ^{31}P NMR (161 MHz, CD_2Cl_2, δ) 138.5 (s). ^{1}H NMR (400 MHz, CD_2Cl_2, δ) 0.95 (m, 1H, CH_2), 1.27 (s, 3H, CH_3), 1.40 (m, 1H, CH_2), 1.42 (b, 2H, CH_2), 1.43 (s, 3H, CH_3), 1.48 (s, 9H, CH_3, *t*-Bu), 1.57 (s, 9H, CH_3, *t*-Bu), 1.79 (s, 3H, CH_3), 1.93 (m, 1H, CH_2), 1.94 (s, 3H, CH_3), 2.32 (s, 3H, CH_3), 2.38 (s, 3H, CH_3), 3.80 (dd, 1H, H5′, $^2J_{5'-5}$ = 11.6 Hz, $^3J_{5'-4}$ = 4.8 Hz), 3.91 (b, 2H, H5, CH═allyl *trans* to S), 4.54 (m, 1H, H4), 4.71 (d, 1H, H2, $^3J_{2-1}$ = 3.6 Hz), 4.95 (dd, 1H, H3, $^3J_{3-P}$ = 15.6 Hz, $^3J_{3-4}$ = 2.4 Hz), 5.03 (m, 1H, CH═allyl *trans* to P), 5.21 (m, 1H, CH═allyl central), 5.85 (d, 1H, H1, $^3J_{1-2}$ = 3.6 Hz), 7.44 (d, 2H, CH═, *J* = 6 Hz), 7.62 (m, 1H, CH═), 7.71 (m, 1H, CH═), 7.78 (m, 2H, CH═), 8.06 (m, 2H, CH═), 8.32 (d, 1H, CH═, *J* = 8.4 Hz). ^{13}C NMR (100 MHz, CD_2Cl_2, δ) 16.3 (CH_3), 16.4 (CH_3), 19.7 (CH_2), 20.0 (CH_3), 20.3 (CH_3), 25.9 (CH_3), 26.3 (CH_3), 26.5 (b, CH_2), 27.5 (CH_2), 31.3 (CH_3, *t*-Bu), 31.4 (CH_3, *t*-Bu), 34.9 (C, *t*-Bu), 35.0 (C, *t*-Bu), 37.6 (C5), 76.5 (d, C4, J_{C-P} = 2.3 Hz), 76.7 (d, C3, J_{C-P} = 3.8 Hz), 82.4 (d, CH═allyl *trans* to S, J_{C-P} = 6.9 Hz), 83.8 (d, C2, J_{C-P} = 3.8 Hz), 103.4 (d, CH═allyl *trans* to P, J_{C-P} = 35.9 Hz), 104.6 (C1), 111.9 (d, CH═allyl central, J_{C-P} = 9.9 Hz), 113.1 (CMe_2), 123.5−144.9 (aromatic carbons). MS HR-ESI [found, 901.2869, $C_{48}H_{60}O_6PPdS$ $(M - BF_4)^+$ requires 901.2878].

Study of the Reactivity of the [Pd(η^3-allyl)(L))]BF_4 with Sodium Malonate by *in Situ* NMR.[27] A solution of *in situ* prepared [Pd(η^3-allyl)(L)]BF_4 (L = phosphite-thioether, 0.05 mmol) in CD_2Cl_2 (1 mL) was cooled in the NMR at −80 °C. At this temperature, a solution of cooled sodium malonate (0.1 mmol) was added. The reaction was then followed by ^{31}P NMR. The relative reaction rates were calculated using a capillary containing a solution of triphenylphosphine in CD_2Cl_2 as external standard.

■ ASSOCIATED CONTENT

Ⓢ Supporting Information

The Supporting Information is available free of charge on the ACS Publications website at DOI: 10.1021/acs.organomet.6b00547.

Copies of ^{31}P{^{1}H} and ^{1}H and ^{13}C{^{1}H} NMR spectra of Pd-intermediates **39**−**43**, reactivity study of Pd-intermediate **39** with sodium malonate. NMR and ee determination details of substitution products **1**−**38** (PDF). (PDF)

Calculated energies and coordinates for all computational structures (PDF)

Computed Cartesian coordinates of all of the molecules reported in this study (XYZ)

■ AUTHOR INFORMATION

Corresponding Authors

*E-mail: Per-Ola.Norrby@astrazeneca.com.

*E-mail: oscar.pamies@urv.cat.

DOI: 10.1021/acs.organomet.6b00547
Organometallics XXXX, XXX, XXX−XXX

*E-mail: montserrat.dieguez@urv.cat.

Notes

The authors declare no competing financial interest.

■ ACKNOWLEDGMENTS

Financial support from the Spanish Government (CTQ2013-40568P), the Catalan Government (2014SGR670), and the ICREA Foundation (ICREA Academia awards to M.D. and O.P.) is gratefully acknowledged.

■ REFERENCES

(1) For reviews, see (a) Tsuji, J. Palladium Reagents and Catalysis, *Innovations in Organic Synthesis*; Wiley: New York, 1995. (b) Trost, B. M.; van Vranken, D. L. *Chem. Rev.* **1996**, *96*, 395−422. (c) Johannsen, M.; Jorgensen, K. A. *Chem. Rev.* **1998**, *98*, 1689−1708. (d) Pfaltz, A.; Lautens, M. In *Comprehensive Asymmetric Catalysis*; Jacobsen, E. N., Pfaltz, A., Yamamoto, H., Eds.; Springer-Verlag: Berlin, 1999; Vol. *2*, Chapter 24. (e) Helmchen, G.; Pfaltz, A. *Acc. Chem. Res.* **2000**, *33*, 336−345. (f) Martin, E.; Diéguez, M. *C. R. Chim.* **2007**, *10*, 188−205. (g) Trost, B. M.; Crawley, M. L. *Chem. Rev.* **2003**, *103*, 2921−2944. (h) Martin, E.; Diéguez, M. *C. R. Chim.* **2007**, *10*, 188−205. (i) Lu, Z.; Ma, S. *Angew. Chem., Int. Ed.* **2008**, *47*, 258−297. (j) Diéguez, M.; Pàmies, O. *Acc. Chem. Res.* **2010**, *43*, 312−322. (k) Trost, B. M.; Zhang, T.; Sieber, J. D. *Chem. Sci.* **2010**, *1*, 427−440. (l) Trost, B. M. *Org. Process Res. Dev.* **2012**, *16*, 185−194.

(2) For selected publications, see (a) Diéguez, M.; Ruiz, A.; Claver, C. *Chem. Commun.* **2001**, 2702−2703. (b) Pàmies, O.; Diéguez, M.; Claver, C. *J. Am. Chem. Soc.* **2005**, *127*, 3646−3647. (c) Pàmies, O.; Diéguez, M. *Chem. - Eur. J.* **2008**, *14*, 944−960. (d) Mata, Y.; Pàmies, O.; Diéguez, M. *Adv. Synth. Catal.* **2009**, *351*, 3217−3234. (e) Mazuela, J.; Pàmies, O.; Diéguez, M. *Chem. - Eur. J.* **2013**, *19*, 2416−2432. (f) Magre, M.; Biosca, M.; Pàmies, O.; Diéguez, M. *ChemCatChem* **2015**, *7*, 114−120. (g) Bellini, R.; Magre, M.; Biosca, M.; Norrby, P.-O.; Pàmies, O.; Diéguez, M.; Moberg, C. *ACS Catal.* **2016**, *6*, 1701−1712. (h) Pàmies, O.; Diéguez, M. *Chem. Rec.* **2016**, DOI: 10.1002/tcr.201600062.

(3) For successful applications, see (a) Evans, D. A.; Campos, K. R.; Tedrow, J. S.; Michael, F. E.; Gagné, M. R. *J. Am. Chem. Soc.* **2000**, *122*, 7905−7920. (up to 98, 90, and 65% ee at −20 °C for **S1**, **S2**, and **S3**, respectively). (b) Nakano, H.; Okuyama, Y.; Hongo, H. *Tetrahedron Lett.* **2000**, *41*, 4615−4618. (up to 94% ee at −30 °C for **S1**). (c) Mancheño, O. G.; Priego, J.; Cabrera, S.; Arrayás, R. G.; Llamas, T.; Carretero, J. C. *J. Org. Chem.* **2003**, *68*, 3679−3686. (up to 97% ee at −20 °C for **S1**). (d) Enders, D.; Peters, R.; Runsink, J.; Bats, J. W. *Org. Lett.* **1999**, *1*, 1863−1866. (up to 97% ee at −20 °C for **S1**). (e) Guimet, E.; Diéguez, M.; Ruiz, A.; Claver, C. *Tetrahedron: Asymmetry* **2005**, *16*, 959−963. (up to 93% ee at 0 °C for **S1**). (f) Caldentey, X.; Pericàs, M. A. *J. Org. Chem.* **2010**, *75*, 2628−2644. (up to 96% ee at rt for **S1**).

(4) Albinati, A.; Pregosin, P. S.; Wick, K. *Organometallics* **1996**, *15*, 2419−2421.

(5) (a) Masdeu-Bultó, A. M.; Diéguez, M.; Martin, E.; Gómez, M. *Coord. Chem. Rev.* **2003**, *242*, 159−201. (b) Pellissier, H. *Tetrahedron* **2007**, *63*, 1297−1330. (c) Mellah, M.; Voituriez, A.; Schulz, E. *Chem. Rev.* **2007**, *107*, 5133−5209. (d) Arrayás, R. G.; Carretero, J. C. *Chem. Commun.* **2011**, *47*, 2207−2211.

(6) Coll, M.; Pàmies, O.; Diéguez, M. *Org. Lett.* **2014**, *16*, 1892−1895.

(7) (a) Dugal-Tessier, J.; Dake, G. R.; Gates, D. P. *Org. Lett.* **2010**, *12*, 4667−4669. (b) Nakai, Y.; Uozumi, Y. *Org. Lett.* **2005**, *7*, 291−293. (c) Feng, B.; Cheng, H.-G.; Chen, J.-R.; Deng, Q.-H.; Lu, L.-Q.; Xiao, W.-J. *Chem. Commun.* **2014**, *50*, 9550−9553.

(8) (a) Deng, W.-H.; Ye, F.; Bai, x.-F.; Zheng, Z.-J.; Cui, Y.-M.; Xu, L.-W. *ChemCatChem* **2015**, *7*, 75−79. (b) Xu, J.-X.; Ye, F.; Bai, X.-F.; Zhang, J.; Xu, Z.; Zheng, Z.-J.; Xu, L.-W. *RSC Adv.* **2016**, *6*, 45495−45502.

(9) (a) Buckingham, J., Ed. *Dictionary of Natural Products*; Cambridge University Press: Cambridge, U.K., 1994. (b) Lumbroso, A.; Cooke, M. L.; Breit, B. *Angew. Chem., Int. Ed.* **2013**, *52*, 1890−1932.

(10) For successful examples of Pd-catalysts, see (a) Trost, B. M.; Shen, H. C.; Dong, L.; Surivet, J.-P. *J. Am. Chem. Soc.* **2003**, *125*, 9276−9277. (b) Trost, B. M.; Toste, F. D. *J. Am. Chem. Soc.* **1998**, *120*, 815−816. (c) Trost, B. M.; Toste, F. D. *J. Am. Chem. Soc.* **1999**, *121*, 4545−4554. (d) Trost, B. M.; Toste, F. D. *J. Am. Chem. Soc.* **2000**, *122*, 11262−11263. (e) Uozumi, Y.; Kimura, M. *Tetrahedron: Asymmetry* **2006**, *17*, 161−166. (f) Tietze, L. F.; Lohmann, J. K.; Stadler, C. *Synlett* **2004**, 1113−1116. For successful applications of Ir-catalysts with phenols, see (g) Shu, C.; Hartwig, J. F. *Angew. Chem., Int. Ed.* **2004**, *43*, 4794−4797. (h) Fischer, C.; Defieber, C.; Suzuki, T.; Carreira, E. M. *J. Am. Chem. Soc.* **2004**, *126*, 1628−1629. (i) López, F.; Ohmura, T.; Hartwig, J. F. *J. Am. Chem. Soc.* **2003**, *125*, 3426−3427. (j) Lyothier, I.; Defieber, C.; Carreira, E. M. *Angew. Chem., Int. Ed.* **2006**, *45*, 6204−6207. (k) Welter, C.; Dahnz, A.; Brunner, B.; Streiff, S.; Dübon, P.; Helmchen, G. *Org. Lett.* **2005**, *7*, 1239−1242. (l) Kimura, M.; Uozumi, Y. *J. Org. Chem.* **2007**, *72*, 707−714.

(11) (a) Iourtchenko, A.; Sinou, D. *J. Mol. Catal. A: Chem.* **1997**, *122*, 91−93. (b) Haight, A. R.; Stoner, E. J.; Peterson, M. J.; Grover, V. K. *J. Org. Chem.* **2003**, *68*, 8092−8096. (c) Lam, F. L.; Au-Yeung, T. T.-L.; Kwong, F. Y.; Zhou, Z.; Wong, K. Y.; Chan, A. S. C. *Angew. Chem., Int. Ed.* **2008**, *47*, 1280−1283. (d) Ye, F.; Zheng, Z.-J.; Li, L.; Yang, K.-F.; Xia, C.-G.; Xu, L.-W. *Chem. - Eur. J.* **2013**, *19*, 15452−15457. (e) Liu, Z.; Du, H. *Org. Lett.* **2010**, *12*, 3054−3057. (f) Kato, M.; Nakamura, T.; Ogata, K.; Fukuzawa, S.-I. *Eur. J. Org. Chem.* **2009**, *2009*, 5232−5238.

(12) (a) Bayardon, J.; Holz, J.; Schäffner, B.; Andrushko, V.; Verevkin, S.; Preetz, A.; Börner, A. *Angew. Chem., Int. Ed.* **2007**, *46*, 5971−5974. (b) Schäffner, B.; Holz, J.; Verevkin, S. P.; Börner, A. *ChemSusChem* **2008**, *1*, 249−253. (c) Schäffner, B.; Schäffner, F.; Verevkin, S. P.; Börner, A. *Chem. Rev.* **2010**, *110*, 4554−4581.

(13) (a) Oslob, J. D.; Åkermark, B.; Helquist, P.; Norrby, P.-O. *Organometallics* **1997**, *16*, 3015−3021. (b) Hagelin, H.; Åkermark, B.; Norrby, P.-O. *Organometallics* **1999**, *18*, 2884−2895.

(14) (a) Hagelin, H.; Svensson, M.; Åkermark, B.; Norrby, P.-O. *Organometallics* **1999**, *18*, 4574−4583. (b) Moberg, C.; Bremberg, U.; Hallman, K.; Svensson, M.; Norrby, P.-O.; Hallberg, A.; Larhed, M.; Csöregh, I. *Pure Appl. Chem.* **1999**, *71*, 1477−1483.

(15) (a) Butts, C. P.; Filali, E.; Lloyd-Jones, G. C.; Norrby, P. O.; Sale, D. A.; Schramm, Y. *J. Am. Chem. Soc.* **2009**, *131*, 9945−9957. (b) Fristrup, P.; Ahlquist, M.; Tanner, D.; Norrby, P.-O. *J. Phys. Chem. A* **2008**, *112*, 12862−12867.

(16) Kleimark, J.; Johansson, C.; Olsson, S.; Håkansson, M.; Hansson, S.; Åkermark, B.; Norrby, P.-O. *Organometallics* **2011**, *30*, 230−238.

(17) (a) Deerenberg, S.; Schrekker, H. S.; van Strijdonck, G. P. F.; Kamer, P. C. J.; van Leeuwen, P. W. N. M.; Fraanje, J.; Goubitz, K. *J. Org. Chem.* **2000**, *65*, 4810−4817. (b) Fernández, F.; Gómez, M.; Jansat, S.; Muller, G.; Martín, E.; Flores Santos, L.; García, P. X.; Acosta, A.; Aghmiz, A.; Giménez-Pedrós, M.; Masdeu-Bultó, A. M.; Diéguez, M.; Claver, C.; Maestro, M. A. *Organometallics* **2005**, *24*, 3946−3956.

(18) (a) Auburn, P. R.; Mackenzie, P. B.; Bosnich, B. *J. Am. Chem. Soc.* **1985**, *107*, 2033−2046. (b) Jia, C.; Müller, P.; Mimoun, H. *J. Mol. Catal. A: Chem.* **1995**, *101*, 127−136. (c) Lehmann, J.; Lloyd-Jones, G. C. *Tetrahedron* **1995**, *51*, 8863−8874. (d) Hayashi, T.; Yamamoto, A.; Ito, Y.; Nishioka, E.; Miura, H.; Yanagi, K. *J. Am. Chem. Soc.* **1989**, *111*, 6301−6311.

(19) (a) Coll, M.; Pàmies, O.; Diéguez, M. *Adv. Synth. Catal.* **2013**, *355*, 143−160. (b) Coll, M.; Pàmies, O.; Diéguez, M. *Chem. Commun.* **2011**, *47*, 9215−9217.

(20) Frisch, M. J.; Trucks, G. W.; Schlegel, H. B.; Scuseria, G. E.; Robb, M. A.; Cheeseman, J. R.; Scalmani, G.; Barone, V.; Mennucci, B.; Petersson, G. A.; Nakatsuji, H.; Caricato, M.; Li, X.; Hratchian, H. P.; Izmaylov, A. F.; Bloino, J.; Zheng, G.; Sonnenberg, J. L.; Hada, M.; Ehara, M.; Toyota, K.; Fukuda, R.; Hasegawa, J.; Ishida, M.; Nakajima, T.; Honda, Y.; Kitao, O.; Nakai, H.; Vreven, T.; Montgomery, J. A., Jr.;

DOI: 10.1021/acs.organomet.6b00547
Organometallics XXXX, XXX, XXX−XXX

Peralta, J. E.; Ogliaro, F.; Bearpark, M.; Heyd, J. J.; Brothers, E.; Kudin, K. N.; Staroverov, V. N.; Kobayashi, R.; Normand, J.; Raghavachari, K.; Rendell, A.; Burant, J. C.; Iyengar, S. S.; Tomasi, J.; Cossi, M.; Rega, N.; Millam, J. M.; Klene, M.; Knox, J. E.; Cross, J. B.; Bakken, V.; Adamo, C.; Jaramillo, J.; Gomperts, R.; Stratmann, R. E.; Yazyev, O.; Austin, A. J.; Cammi, R.; Pomelli, C.; Ochterski, J. W.; Martin, R. L.; Morokuma, K.; Zakrzewski, V. G.; Voth, G. A.; Salvador, P.; Dannenberg, J. J.; Dapprich, S.; Daniels, A. D.; Farkas, O.; Foresman, J. B.; Ortiz, J. V.; Cioslowski, J.; Fox, D. J. *Gaussian 09*, revision A.02; Gaussian, Inc.: Wallingford, CT, 2009.

(21) (a) Lee, C.; Yang, W.; Parr, R. G. *Phys. Rev. B: Condens. Matter Mater. Phys.* **1988**, *37*, 785−789. (b) Becke, A. D. *J. Chem. Phys.* **1993**, *98*, 5648−5652.

(22) Hay, P. J.; Wadt, W. R. *J. Chem. Phys.* **1985**, *82*, 299−310.

(23) (a) Hehre, W. J.; Ditchfield, R.; Pople, J. A. *J. Chem. Phys.* **1972**, *56*, 2257−2261. (b) Hariharan, P. C.; Pople, J. A. *Theor. Chim. Acta* **1973**, *28*, 213−222. (c) Francl, M. M.; Pietro, W. J.; Hehre, W. J.; Binkley, J. S.; Gordon, M. S.; Defrees, D. J.; Pople, J. A. *J. Chem. Phys.* **1982**, *77*, 3654−3665.

(24) (a) Miertus, S.; Tomasi, J. *Chem. Phys.* **1982**, *65*, 239−245. (b) Mennucci, B.; Tomasi, J. *J. Chem. Phys.* **1997**, *106*, 5151−5158. (c) Cossi, M.; Barone, V.; Mennucci, B.; Tomasi, J. *Chem. Phys. Lett.* **1998**, *286*, 253−260.

(25) (a) Krishnan, R.; Binkley, J. S.; Seeger, R.; Pople, J. A. *J. Chem. Phys.* **1980**, *72*, 650−654. (b) McLean, A. D.; Chandler, G. S. *J. Chem. Phys.* **1980**, *72*, 5639−5648.

(26) (a) Grimme, S.; Antony, J.; Ehrlich, S.; Krieg, H. *J. Chem. Phys.* **2010**, *132*, 154104. (b) Grimme, S.; Ehrlich, S.; Goerigk, L. *J. Comput. Chem.* **2011**, *32*, 1456−1465.

(27) van Haaren, R. J.; Keeven, P. H.; van der Veen, L. A.; Goubitz, K.; van Strijdonck, G. P. F.; Oevering, H.; Reek, J. N. H.; Kamer, P. C. J.; van Leeuwen, P. W. N. M. *Inorg. Chim. Acta* **2002**, *327*, 108−115.

DOI: 10.1021/acs.organomet.6b00547
Organometallics XXXX, XXX, XXX−XXX